

## PROTON RADIOACTIVITY IN LIGHT RARE-EARTH DEFORMED NUCLEI

M. IVASCU<sup>1</sup>, I. CATA-DANIL<sup>1</sup>, D. BUCURESCU<sup>1</sup>, GH. CATA-DANIL<sup>1</sup>, L. STROE<sup>1</sup>,  
F. SORAMEL<sup>2</sup>, C. SIGNORINI<sup>3</sup>, A. GUGLIELMETTI<sup>4</sup>, R. BONETTI<sup>4</sup>

<sup>1</sup> NIPNE, P.O. Box MG-6, R.O. – 077125 Bucharest – Măgurele, Romania

<sup>2</sup> Dipartimento di Fisica and INFN, University of Udine, via delle Scienze 208

<sup>3</sup> Dipartimento di Fisica and INFN, University of Padova, I-35131 Padova, Italy

<sup>4</sup> Istituto di Fisica Generale and INFN, University of Milano, I-20133 Milano, Italy

(Received 11 July, 2005)

*Abstract.* For several years, in the frame of an international coloboration we have started a program to study exotic decays at the proton drip-line with special attention to proton radioactivity in the light rare earth region. The theoretical calculations stressed the fact that p- emitting nuclei with  $54 < Z < 64$  are expected to be very deformed in their ground state and for this reason their study is an important test for the theoretical models that describe proton radioactivity. The decay by proton emission of the  $^{117}\text{La}$  nucleus has been studied *via* the 310 MeV  $^{58}\text{Ni} + ^{64}\text{Zn}$  reaction. For this nucleus two levels that decay to the ground state of  $^{116}\text{Ba}$  with  $E_p = 783(6)$  keV [ $T_{1/2} = 22(5)$  ms] and  $E_p = 933(10)$  keV [ $T_{1/2} = 10(5)$  ms ] have been discovered. Calculations performed for a deformed proton emitter reproduce quite well the experimental results confirming that  $^{117}\text{La}$  is strongly deformed. A search for proton radioactivity of  $^{123}\text{Pr}$  using a  $^{58}\text{Ni}$  beam (260–300 MeV) and  $^{70}\text{Ge}$  target has been done. The same setup for measuring the p-decay of  $^{117}\text{La}$  and  $^{123}\text{Pr}$  was used to investigate a possible decay *via* proton emission of the odd-odd nucleus  $^{126}\text{Pm}$ . We performed analysis of the deformed proton emitter  $57 \leq Z \leq 69$  by using Möller *et al.* and Relativistic Hartree – Bogoliubov models concerning the location of proton drip-line, the separation energies for proton separation and ground-state quadrupole deformations.

*Key words:* proton radioactivity, deformed nuclei, rare-earth nuclei.

### INTRODUCTION

One of the most exciting subjects in contemporary nuclear physics is the search for the nuclear limits of stability. The knowledge of nucleon emission from ground state of spherical as well as deformed nuclei provides information on these limits.

The study of these limits is very important, since it provides a unique tool to get spectroscopic information on nuclei far away from the stability valley. From the theoretical point of view these studies permit a stringent test on models of the nuclear mean field and their dependence on isospin. Because of the strongly repulsive Coulomb force the number of isotopes with proton excess is much more

limited than the number of isotopes with neutron excess. Therefore, in contrast to the neutron drip line, which today is experimentally known only up to  $Z = 17$ , the location of the proton drip line is today well investigated for isotopes with odd proton numbers up to  $Z = 91$ . The region of proton rich nuclei is of special interest because of several reasons a) Proton radioactivity provides a new and very precise experimental tool to investigate details of nuclear structure at the edge of the nuclear stability, b) the  $N = Z$  line, which is interesting for a number of theoretical reasons comes close to the proton drip line around  $N = 50$  and passes it afterwards, c) the mass region  $60 < A < 100$  is important for the process of nucleosynthesis during explosive hydrogen burning, d) at the present time the unified theory gives the possibility to interpret the results of a considerable amount of experimental data on nuclei with  $50 < Z < 84$ . It has been demonstrated that this theory has given the unique information about the structure and shapes of the proton decaying nuclei. Recently many proton emitters with  $Z > 50$  have been found and their decay properties determined [1, 2]. In this condition the proton drip line is readily delineated, above  $Z = 50$ , by nuclei which decay by the emission of a proton. So-called proton emitters have been identified in almost all odd –  $Z$  systems from Sb ( $Z = 51$ ) to Bi ( $Z = 83$ ). In most cases, proton emission is understood in terms of simple quantum tunnelling through a one-dimensional barrier in a spherical nucleus. Hence, proton decay has become a potent spectroscopic tool to characterize states located near the Fermi surface in nuclei at the very limits of stability. First examples of p emitters, produced *via* (p, 2n) and (p, 3n) evaporation channels and located in the region  $68 < Z < 82$  have been interpreted by means of simple WKB calculations as being spherical. However, in the region  $50 < Z < 67$  the predicted p emitters are expected to be quite deformed in their ground state due to the complexity of the emitted proton wave function. Moreover, while many spherical p-emitters are connected with other nuclei through  $\alpha$  decay chains, in the deformed region  $\alpha$  decay is rather uncommon and only a very restricted group of nuclei has measurable  $\alpha$  decay branch. This implies that in the  $50 < Z < 67$  region one cannot use the daughter and granddaughter  $\alpha$  decay to tag the proton decay.

A complete explanation of the p emission process should be able to describe this decay as a function of the deformation parameter. Thus it is very important to study and characterize the p emission from deformed nuclei in order to fine tune the theoretical description of this process.

First experiments on  $^{109}\text{I}$  [4],  $^{112,113}\text{Cs}$  [4–6] performed at Munich and Daresbury pointed out that for these transitional nuclei an interpretation as spherical nuclei is not enough. Indeed, calculations including the deformation parameter  $\beta_2$  [7, 8] have been able to give a coherent description of these nuclei. Proton radioactivity was recently observed in  $^{141}\text{Ho}$  and  $^{131}\text{Eu}$  [9]. Based on the measured half-lives, the proton emitting states were interpreted as requiring the presence of a sizable quadrupole deformation [7]. In  $^{131}\text{Eu}$ , additional information

was obtained by observing not only proton decay to the ground state of the daughter nucleus  $^{130}\text{Sm}$  but also to the first excited  $2^+$  level. By utilizing both the excitation energy of the  $2^+$  state and the branching ratio, the spin and intrinsic configuration of the proton emitting state was unambiguously determined. In  $^{141}\text{Ho}$  no such decay to the  $2^+$  level has been observed and the assignment of the  $7/2^-$  [523] and  $1/2^+$ [411] Nilsson configuration to the  $^{141}\text{Ho}$  ground and isomeric state, respectively, was deduced solely from the measured decay rates. Confirmation of sizable deformation as well as complementary information on the structure of these states was obtained from in-beam  $\gamma$ -ray studies utilising the Recoil Decay Tagging (RDT). All the proton emitters below  $^{131}\text{Eu}$  with  $Z > 54$  are expected to have strongly deformed ground states, among them  $^{117}\text{La}$ ,  $^{123}\text{Pr}$  and  $^{126}\text{Pm}$  are predicted to have  $\beta_2 \approx 0.3$  [3]. For this reason we decided to study these nuclei.

## EXPERIMENT

The measurements of  $^{117}\text{La}$ ,  $^{123}\text{Pr}$  and  $^{126}\text{Pm}$  decay by proton emission have been carried out at the Legnaro National Laboratories. The reactions were:  $^{64}\text{Zn}(^{58}\text{Ni}, p4n)^{117}\text{La}$  at 310 MeV, with a  $1 \text{ mg/cm}^2$  self-supporting target;  $^{58}\text{Ni}(^{70}\text{Ge}, p4n)^{123}\text{Pr}$  at 290 MeV, with a  $500 \text{ }\mu\text{g/cm}^2$  self-supporting target; and  $^{74}\text{Se}(^{58}\text{Ni}, p5n)^{126}\text{Pm}$  at 425 MeV, with a  $1 \text{ mg/cm}^2$  self-supporting target, respectively. The beam was delivered by the Tandem + LINAC accelerator of Legnaro with an average intensity of 1.5 pA. The experimental setup (Fig. 1) used the Recoil Mass Spectrometer (RMS) with its maximum solid angle acceptance (10 msr), together with a DSSD (double sided silicon strip detector) (Fig. 2) situated one meter downstream of the RMS focal plane. Based on the RMS  $A/q$  selectivity, the spatial and energy information given by the DSSD and an absolute clock (4 MHz), it is possible to measure the decay properties of nuclei with half-lives between 50  $\mu\text{s}$  and a few seconds.

Among all the recoils focused on the RMS focal plane, only those falling in the range  $(A - 1)/q - (A + 1)/q$  with respect to the central  $A/q$  path are implanted in the DSSD. The DSSD has  $(40 \times 40)$  strips 1 mm wide, and a thickness of 60  $\mu\text{m}$ . To reduce the high recoil energy that would saturate the amplifiers, a degrader foil of  $2 \text{ mg/cm}^2$  natural Ni was inserted in front of the DSSD. The DSSD signals are treated differently on the two sides; in the vertical direction (x side) strips are acquired separately to get both position and energy information, while in the horizontal direction (y side) all strips are read together through a delay line (2 ns per strip). Preamplifiers for vertical strips are hosted in the detector chamber. Cooling of both detector and preamplifier supports is guaranteed by Pellier elements with water circulation. Acquired events were those that produce at least one signal on the x side of the DSSD.

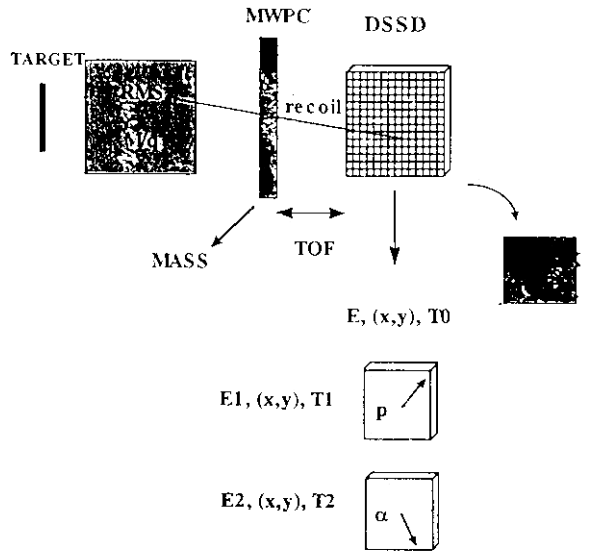


Fig. 1 – The experimental setup.

- ☆  $\Omega_{RMS} = 10 \text{ msr}$
- ☆ Exit window after MWPC (14\*70)mm<sup>2</sup>
- ☆ Only one charge state and one mass can reach the DSSD
- ☆  $d_{MWPC-DSSD} \sim 1\text{m}$

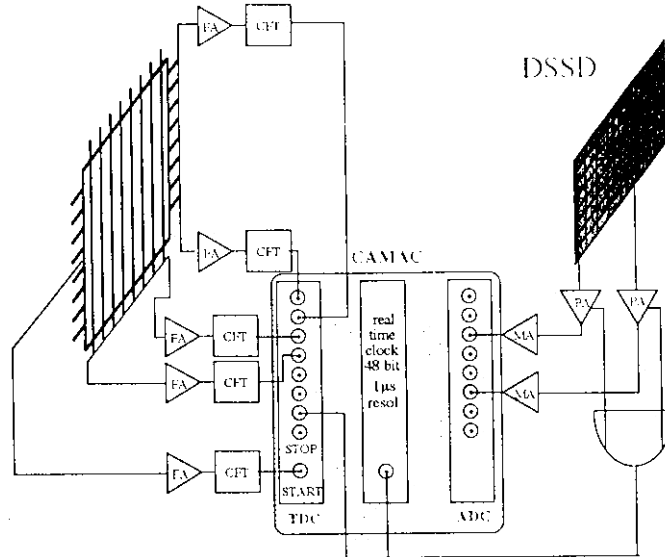


Fig. 2 – Double sided silicon strip detector.

Due to the low cross section especially for  $^{123}\text{Pr}$  and  $^{126}\text{Pm}$ , data analysis requires stringent cuts on the measured parameters to enhance the proton events with respect to the background. Therefore we conditioned all decay events with an anti-coincidence signal from a veto detector positioned behind the DSSD; the veto detector [a (4 x 4) mm<sup>2</sup> Si detector] collects decay events which did not stop inside the DSSD (whose thickness is only 60  $\mu\text{m}$ ), but released only a part of their energy in it contributing to the strong background at  $E_{\text{decay}} = 1 \text{ MeV}$ , *i.e.*, in the energy region where proton events are expected. Beside this general condition we could clean our data acting on other two parameters, namely TOF between the focal plan detector (MWPC) and the DSSD, and the recoil mass signal coming from the MWPC. The TOF signal allows separation of recoil events from scattered beam event, while the MWPC recoil mass signal allows selection of recoils on the  $A/q$  basis.

Last, we could select the decay events according to the time passed from the recoil implantation in a specific DSSD cell.

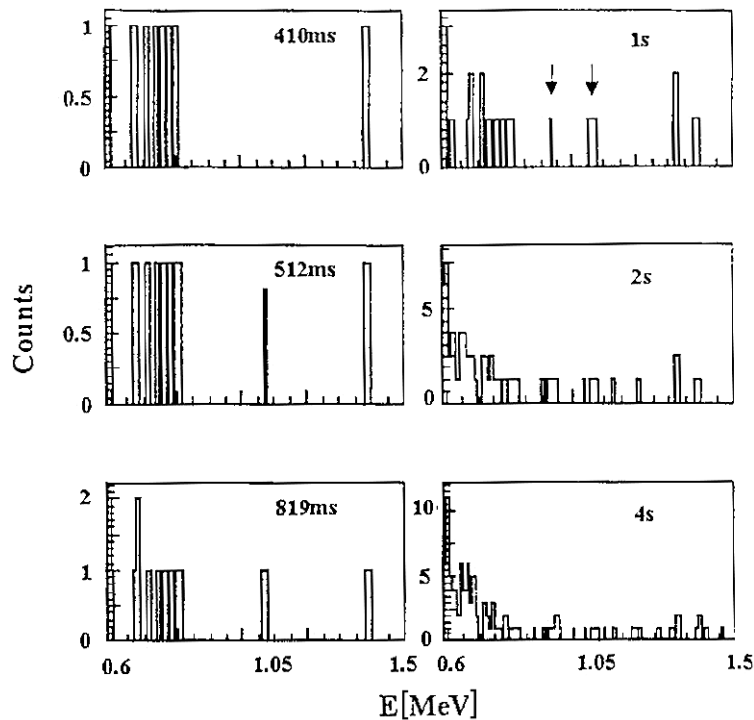


Fig. 3 – Experimental decay spectra for  $^{126}\text{Pm}$ . Different spectra correspond on different time between the recoil implantation event and the decay event. The time gates are all starting at zero. All spectra are in anti-coincidence with the veto detector and correspond to recoil events requiring TOF and mass 126 conditions.

Fig. 3 shows the time evolution of the low energy part of decay events spectrum in correspondence to gate  $A/q = 126/36^+$  and requiring both anti-coincidence with the veto detector and a TOF signal corresponding to recoils.

DSSD energy calibration was obtained from an  $\alpha$  source with three peaks, a pulser signal, and a known p decay. The latter one was, in all our experiments, the  $^{147}\text{Tm}$  p decay which presents two proton lines (1.051 MeV and 1.131 MeV) and was produced after (p,2n) evaporation from the fusion reaction  $^{58}\text{Ni} + ^{92}\text{Mo}$  ( $E_{\text{beam}} = 261$  MeV) that was shortly run before the main experiment.

Fig. 4 gives an example of data from the calibration run on  $^{147}\text{Tm}$ . Decay events in a time window of (0–1) s from the last recoil registered in the same strip are shown. The low energy peak is the ground state proton decay of  $^{147}\text{Tm}$  which has a half-life of 560 ms. Other peaks correspond to  $\alpha$  decays of nuclei produced in the reaction between the beam and the Mo isotopes with  $A \neq 92$  present in our target. All these well-known peaks have been used for internal energy calibration of the DSSD. Using shorter time gates the proton line from the decay of the excited 11/2<sup>-</sup> level of  $^{147}\text{Tm}$  (1.11 MeV and 360  $\mu\text{s}$ ) clearly appears in the spectrum.

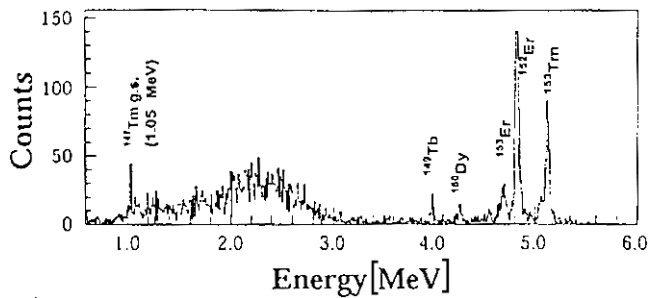


Fig. 4 – Decay events from the  $^{58}\text{Ni} + ^{92}\text{Mo}$  reaction leading to the known p-emitter  $^{147}\text{Tm}$ . All the events collected in the DSSD corresponding to  $A/q = 147/27^+$  recoils and occurring in a time interval of 1 s after a recoil implantation in a given strip are shown. The 1.05 MeV peak corresponds to the ground state p decay of  $^{147}\text{Tm}$ , other lines come from  $\alpha$  decays of indicated isotopes.

## RESULTS

### $^{117}\text{La}$

During the  $^{117}\text{La}$  run RMS fields were chosen to focus  $A = 117$  and  $q = 30^+$  recoils. Fig. 5 shows the data from the  $^{58}\text{Ni} + ^{64}\text{Zn}$  reaction. Panel (a) presents all decay events in the DSSD. Already from this spectrum, with no time or mass selection, a peak is emerging at  $\approx 800$  keV. The peak becomes evident in panel (b) where a time requirement of  $\Delta t \leq 100$  ms between the implanted recoil and the subsequent decay event has been imposed. Finally, in panel (c) a further condition has been added on the recoils  $A/q$  value ( $A/q = 117/30^+$ ); the peak at 783(6) keV becomes more and more pronounced by increasing the number of conditions. Therefore this peak is attributed to the decay by proton emission of  $^{117}\text{La}$  ground

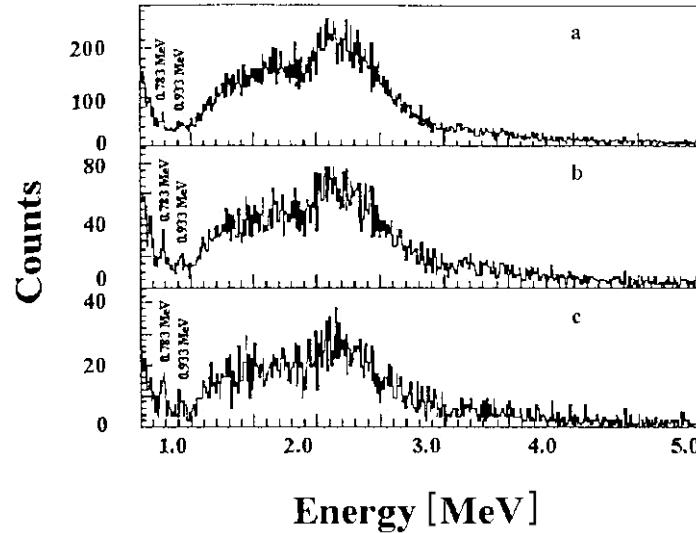


Fig. 5 – Decay events in the DSSD during the 310 MeV  $^{58}\text{Ni} + ^{64}\text{Zr}$  run. Fig. 2a shows all the decays. Fig. 2b displays decay events occurring in a 100 ms time interval after a recoil implantation in a given strip. In Fig. 2c an additional condition  $M/q = 117/30^+$  for the recoils is required.

state to the ground state of  $^{116}\text{Ba}$ ; all other possibilities are ruled out since they correspond to nuclei closer to the stability line than  $^{117}\text{La}$  and therefore with much lower probability to decay by p emission. In addition, considering an overall RMS transmission of 5–10%, a 60% efficiency for the DSSD and the 75 events detected for this decay, a cross section of  $\approx 200$  nb for the  $^{117}\text{La}$  ground state is deduced, in good agreement with other experimental cross section for (p,4n) evaporation channels leading to p emitters in this deformed region.

From the experimental value of  $E_p = 783(6)$  keV, a  $Q_p$  – value of  $790(6)$  keV is obtained. Proton peak time analysis, illustrated in Fig. 5 together with its fit, results in  $T_{1/2} = (20 \pm 5)$ ms. However, since the recoil counting rate per strip during the experiment was 5 Hz, the possibility of correlating a decay event to a wrong recoil in the same strip has the effect of lowering the level half-life by 10%. After this correction the experimental half-life for this decay becomes  $T_{1/2}(22 \pm 5)$  ms).

In Figs. 5(b) and 5(c) a second proton peak can be seen in the region immediately above 900 keV. Though it is not a high statistics peak, its analysis gives positive results, the peak turns out to correspond to  $E_p = (933 \pm 10)$  keV and  $T_{1/2} = (10 \pm 5)$  msec (including the random coincidence correction). After the usual corrections a  $Q_p = (941 \pm 10)$  keV is deduced. This second peak is populated with  $\sim 1/3$  of the 783 keV peak cross section. The time analysis of the peak is shown in Fig. 6(a). Experimental data do not show evidence for  $\alpha$  lines which might come from  $^{117}\text{La}$  decay.

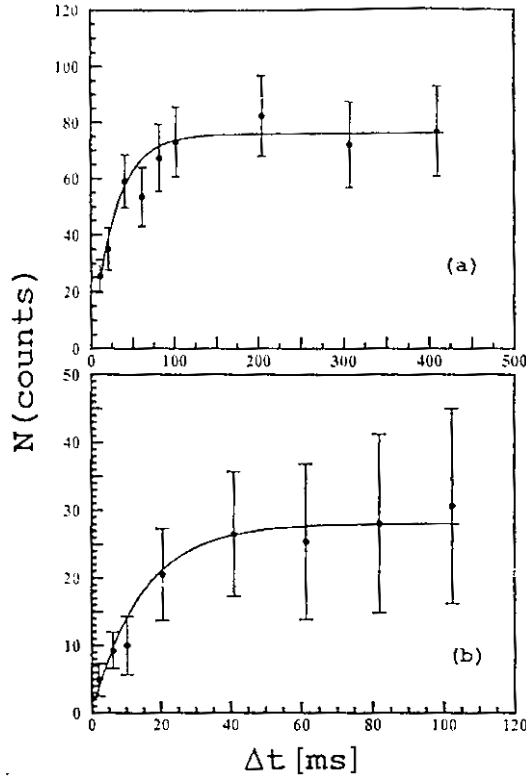


Fig. 6 – Time analysis of the 783 keV (a) and 933 keV (b) proton peaks of  $^{117}\text{La}$ .

It can be seen that both experimental  $Q$  values lie in between the range determined by existing mass predictions and calculations. Audi and Wapstra [11] give  $Q_p = (471 \pm 1021)$  keV; Möller and Nix [3] predict  $Q_p = 501$  keV; Liran and Zeldes [12]  $Q_p = 1011$  keV; and Jänecke and Masson [13]  $Q_p = 1021$  keV.

From Ref. [3] the  $^{117}\text{La}$  nucleus should be strongly deformed with  $\beta_2 = 0.29$  and  $\beta_4 = 0.1$  and calculations for proton emission from a spherical nucleus should be used to fix a range for the possible half-lives. With a code [14] based on a simple WKB spherical model the  $Q_p^{\text{nucl}} = 800$  keV (which results from the sum of  $Q_p$  value and 10 keV electron screening effect) should correspond either to  $T_{1/2} = 0.33$  ms if the ground state were a  $d_{5/2}$  or to  $T_{1/2} = 110$  ms if it were a  $g_{7/2}$  level, these being the only candidates for the ground state configuration of  $^{117}\text{La}$  in the spherical approximation.

A calculation which is able to take into account the ground state deformation was necessary to understand  $^{117}\text{La}$  structure. Using the model of Maglione *et al.* [8] which assumes that the emitted proton is moving in a deformed single particle Nilsson level and its wave function is obtained by solving exactly the Schrödinger equation for a deformed Woods-Saxon potential with a deformed spin-orbit term

and realistic parameters, it is possible to establish the  $^{117}\text{La}$  Fermi Surface. At large deformation ( $\beta_2 = 0.3$  and  $\beta_4 = 0.1$ ) the ground state is likely a  $K = 3/2^+$  state coming from the spherical level.

Fig. 7(a) shows the result obtained by performing a calculation for this level using the method of Ref. [8]. The calculation includes the  $Q_p$  experimental error (gray band) and the spectroscopic factor estimated as in [15–16]; the spectroscopic factor turns out to be  $0.6 \pm 0.1$  for deformations  $\beta_2 = (0.2-0.4)$ . The agreement with the experimental results is good for  $\beta_2 > 0.16$  with  $\beta_4 = \beta_2/3$ .

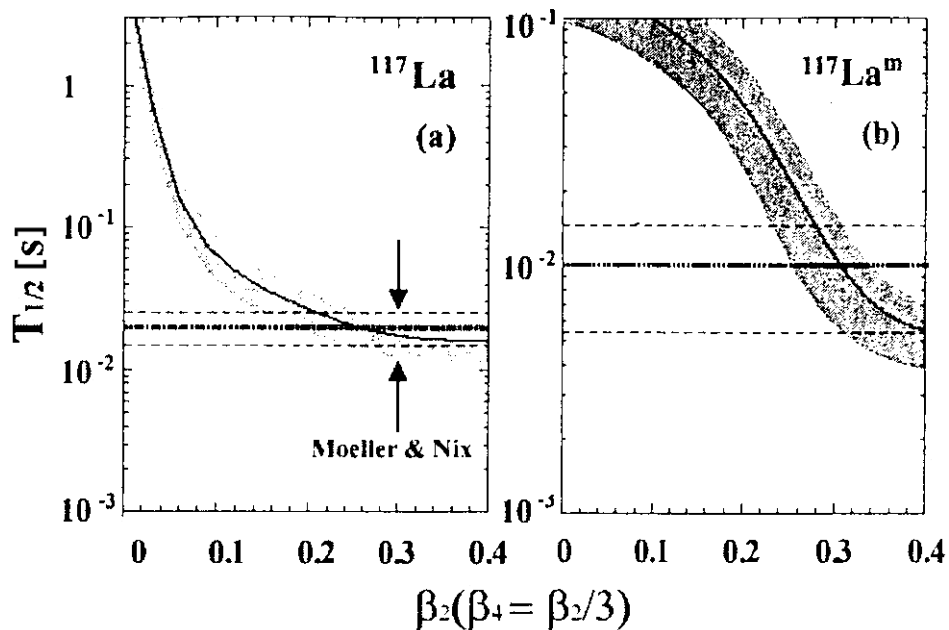


Fig. 7 – Calculated proton partial half-life as a function of the deformation parameter for 783 keV (a) and 933 keV (b) proton decay levels of La. Gray bands reflect the experimental error for the  $Q_p^{\text{nucl}}$  values, while the horizontal dashed lines correspond to the experimental errors for the half-lives. For the ground state decay the value obtained from Ref. [3] is also indicated.

Similar calculations performed for the second peak, assuming that this proton is emitted from a  $K = 9/2^+$  state coming from the  $g_{9/2}$  spherical level, give the result of Fig. 7(b): the agreement with experimental data is quite good also in this case, and the deformation for the level emitting the 933 keV is  $\beta_2 > 0.24$  (always with  $\beta_4 = \beta_2/3$ ).

It is worth noting that negative parity states originating from the spherical  $h_{11/2}$  level, though lying close to the Fermi surface, do not reproduce the data in either case.

At this point a few words on the relative population of the two proton decaying levels are necessary. In fact one expects that the higher spin level, being yrast, would have a higher population than the ground state, opposite to the experimental observation. Two different explanations are possible. The  $h_{11/2}$  band is the yrast band in neutron deficient Cs, La, Pr nuclei, and its decay might feed the  $3/2^+$  band. This would explain our results on the proton intensities. However, there is a second possibility of an M3 transition from the  $9/2^+$  to the  $3/2^+$  state competing with the  $9/2^+$  proton decay. This transition is indeed observed in  $^{112}\text{Cs}$ . For  $^{117}\text{La}$  a 150 keV M3 transition would have a partial half-life of  $\sim 3.5$  s (Weisskopf estimate corrected for internal conversion). Taking into account that maximum enhancement for an M3 is 10 [17], the partial half-life becomes 350 ms, *i.e.*, 35 times slower than the experimental  $9/2^+$  half-life. This result rules out the second possibility.

Concluding, we have found that  $^{117}\text{La}$  has two p-decaying levels that populate the ground state of  $^{116}\text{Ba}$ : the ground state with  $J^\pi = 3/2^+$  decays *via* a  $(783 \pm 6)$  keV proton with  $T_{1/2} = (22 \pm 5)$  ms, while the excited level decay, with  $E_x = 151(12)$  keV (this value corresponds to the difference between the  $Q_p$  values) and  $J^\pi = 9/2^+$ , is characterized by  $E_p = (993 \pm 10)$  keV and  $T_{1/2} = (10 \pm 5)$  ms. Since the data do not show evidence of  $\alpha$  decays, and since a possible  $\beta$  decay would have  $T_{1/2}^\beta \sim 338$  ms [18] we attribute 100% branching to each of the two p decays. In addition  $^{117}\text{La}$  is quite deformed in agreement with what is expected from [3].

In summary, the decay by proton emission of the proton rich  $^{117}\text{La}$  nucleus has been studied, characterizing the energy and the half-lives of the two experimentally measured decays, and determining spin, parity and deformation of the decaying levels.

### **$^{123}\text{Pr}$**

As was stressed before, research on proton radioactivity is a way to get information on nuclei at the p-drip line, for which fusion evaporation cross section are  $< 1$  mb. Results on new p emitters are now available for many nuclei with  $Z \geq 50$  up to  $Z = 83$ : in fact, recent experiments [1, 2, 5, 6, 21] performed at the Argonne National Laboratory, have identified p-emitters nuclei with  $Z \geq 50$  up to  $Z = 83$ , but for odd-  $Z$  nuclei with  $Z = 57-67$  information is scarce. Proton radioactive nuclei in the region between barium and erbium are predicted to be deformed (Fig. 18). At deformation between 0.2 and 0.3 the relevant Nilsson orbitals for the protons have the asymptotic quantum numbers (with  $57 \leq Z \leq 67$ )  $1/2^-$ [550],  $3/2^-$ [451],  $5/2^-$ [532],  $3/2^+$ [411] and  $7/2^-$ [523]. Except for the last orbital, low – spin values are expected, and for the proton transitions to daughter nuclei with similar deformations, hindrance factors for bigger changes of angular momenta do not occur, especially because low-lying rotational levels can be

populated. In the  $^{32}\text{S} + ^{96}\text{Ru} \rightarrow ^{128}\text{Nd}$  reaction investigated by Karnaukhov *et al.* [22] deformed nuclei in this region were produced. To estimate the partial proton half-life, the WKB method and assumed spherical nuclei have been used [23]. Assuming  $^{121}\text{Pr}$  as proton emitter, the calculated partial proton half-lives are 48  $\mu\text{sec}$  ( $\Delta\ell = 0$ ), 520  $\mu\text{sec}$  ( $\Delta\ell = 2$ ) for 0.83 MeV proton and 1.6 nsec ( $\Delta\ell = 2$ ) for 1.2 MeV protons.

A rough estimate for the line in the (Z,N) plane of proton radioactive nuclei between cesium and thulium with partial half-lives within an experimental window of about 1  $\mu\text{sec}$  to 1 sec can be obtained by fitting a straight line through known proton emitters  $^{109}\text{I}$ ;  $^{113}\text{Cs}$ ;  $^{117}\text{La}$ ;  $^{131}\text{Eu}$ ;  $^{139}\text{Ho}$ ;  $^{147}\text{Tm}$  and  $^{151}\text{Lu}$  with  $N = 1.375Z - 17.2$  (Fig. 18). We obtain as candidates for proton radioactivity the nuclei  $^{118}\text{La}$ ;  $^{124}\text{Pr}$ ;  $^{128}\text{Pm}$ ;  $^{132}\text{Eu}$ ,  $^{137}\text{Tb}$  and  $^{142}\text{Ho}$  and their neighboring isotopes with  $\Delta N = \pm 1$ . Except for the  $\beta$  delayed proton emitter  $^{124}\text{Pr}$  none of these 18 nuclei have been identified so far, which confirms the fact that the proton drip-line is shifted to lower N value. Nevertheless, search experiments, must be continued and, with higher sensitivity of experiment, one can hope that ground state or isomeric state proton radioactivity will also be established in this region.

As a consequence, it was quite important to have experimental information on light rare earth nuclei the p – drip line and in particular on Pr (Z = 59) isotopes. Proton-rich Pr nuclei can be reached with two different beam-target combinations, leading to the same compound nucleus ( $^{128}\text{Nd}$ ):  $^{58}\text{Ni} + ^{70}\text{Ge}$  and  $^{32}\text{S} + ^{96}\text{Ru}$ . The candidate for p-emission is  $^{123}\text{Pr}$  which can be obtained by the (p4n) evaporation channel.

Cascade calculations give for the first reaction a maximum cross section of 25  $\mu\text{b}$  with a 290 MeV  $^{58}\text{Ni}$  beam (such calculations are performed using calculated masses from Jänecke and Masson [13] where experimental values are not available). We performed the study of p-decay of  $^{123}\text{Pr}$  using the RMS together with a DSSD after its focal plane: RMS selects a beam of recoils of a specific M/q value which are then implanted in the silicon detector. With the subsequent recoil decay it is possible to correlate the decay event with its mother.

In this condition we run a first experiment aimed to search for p-radioactivity of  $^{123}\text{Pr}$ . The total yield on DSSD, selecting a specific M/q value (123/57) was about 7,000 events/s by using a 1 mg/cm<sup>2</sup> thick target and an I = 5 pA beam (this because for each value of M produced at least three different nuclear species, and RMS cannot distinguish between similar M/q values corresponding to different masses; since this beam illuminated about 1000 cells of the DSSD, we can be able to measure decay half-lives up to 100 ms (as a reference point one can consider the measured half-lives of  $^{109}\text{I}$  and  $^{112,113}\text{Cs}$  which are between 10 and 500  $\mu\text{s}$ ).

For the p-decay, taking into account that the DSSD has a 50% efficiency (due to its geometry) we expected to have 1000 proton events per hour, if the measured cross section was close to the calculated one and if the p-decay should be main

decay mode of  $^{123}\text{Pr}$  (we can again quote the results obtained for I and Cs nuclei which have been produced after pxn evaporation with cross sections ranging from 10  $\mu\text{b}$  to 0.5  $\mu\text{b}$ ).

In order to optimize the  $^{123}\text{Pr}$  yield we planned to measure a three point excitation function with  $^{58}\text{Ni}$  beams from 260 up to 300 MeV.

Unfortunately, the results are not conclusive; despite the better statistics, experimental set-up and running conditions, no evidence was found for the 800 keV proton peak proposed by Bogdanov [24].

Also for  $^{121}\text{Pr}$  the studies did not report any proton emission, which confirms again the fact that proton drip-line is shifted to the lower N value.

### **$^{126}\text{Pm}$**

The RMS fields during this experiment were set for a central trajectory with  $A = 126$  and  $q = 36^+$ . As usual, prior to the run, we calibrated in energy the DSSD strips using the very-well known case of the  $^{147}\text{Tm}$ .

Due to the low cross section, the  $^{126}\text{Pm}$  data analysis requires stringent cuts on the measured parameters to enhance the proton events with respect to the background. Therefore we conditioned all decay events with an anti-coincidence signal from a veto detector positioned behind the DSSD .

Unfortunately, the result cannot be conclusive: Fig. 3 shows some possible candidates at  $E_p \sim 900$  keV and 1100 keV. They have different half-lives, but in both cases they are too long ( $> 1$  s) in comparison with the  $\beta$ -decay half-life which is expected to be around 200 ms. On the other hand the expected events are only 10 and the odd-odd nature of  $^{126}\text{Pm}$  together with a strong deformation might open more than one decay channel, spreading the total cross section on several channels.

## **ROTATIONAL BANDS IN LIGHT RARE-EARTH DEFORMED PROTON EMITTER**

In general, before any experiment, it is necessary to calculate one-proton separation energies  $S_p(Z, N)$ . In Fig. 8 we display our calculated one-proton separation energies for odd-Z nuclei  $57 \leq Z \leq 69$ , as a function of the neutron number by using the model of P. Möller *et al.* [18]. One can see that there are more than 41 isotopes with negative  $S_p$  value but only for  $^{117}\text{La}$ ;  $^{126}\text{Pm}$ ;  $^{131}\text{Eu}$ ;  $^{141}\text{Ho}$ ;  $^{145}\text{Tm}$  and  $^{146}\text{Tm}$  one has experimental measurements.

Similar calculations performed by using Relativistic Hartree – Bogoliubov model [20] for the odd-Z nuclei  $59 \leq Z \leq 69$ , as a function of the number of neutron are displayed in Fig. 9. The model predicts the drip-line nuclei :  $^{124}\text{Pr}$ ;  $^{129}\text{Pm}$ ;  $^{134}\text{Eu}$ ;  $^{139}\text{Tb}$ ;  $^{146}\text{Ho}$  and  $^{152}\text{Tm}$ . In heavy proton drip-line nuclei the potential energy barrier, which results from the superposition of the Coulomb and centrifugal potential, is relatively high.

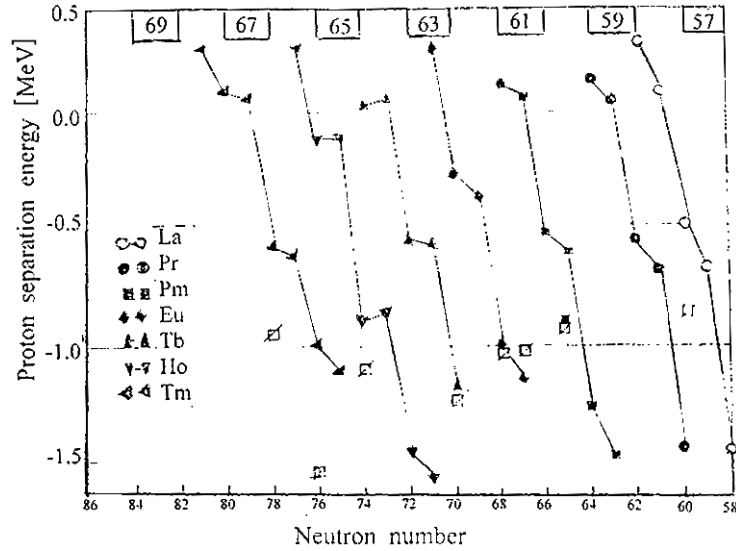


Fig. 8 – Calculated one-proton separation energies for odd-Z nuclei  $57 \leq Z \leq 69$  at and beyond the drip-line.

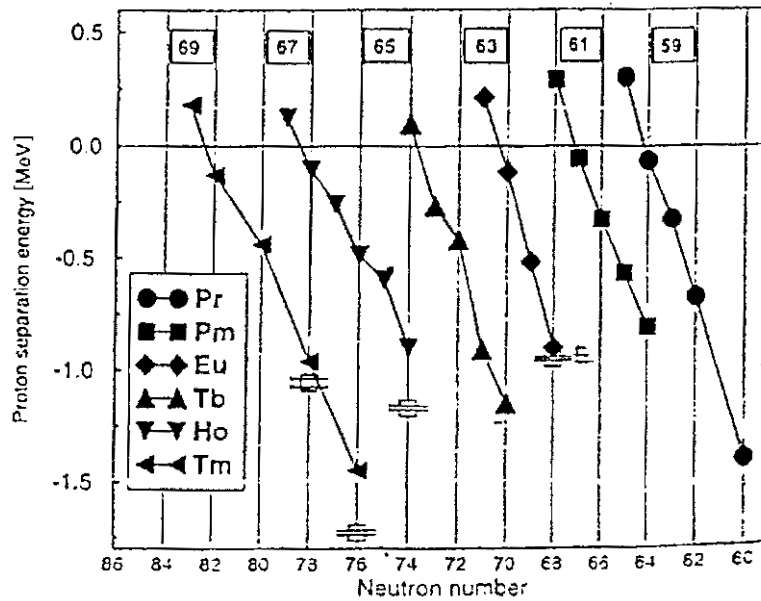


Fig. 9 – Calculated one-proton separation energies for odd-Z nuclei  $59 \leq Z \leq 69$  at and beyond the drip-line.

The calculated separation energies should be compared with reported experimental data on proton radioactivity from  $^{131}\text{Eu}$ ;  $^{141}\text{Ho}$ ;  $^{145}\text{Tm}$  and  $^{147}\text{Tm}$ .

Proton emission from deformed nuclei has been one of the focal points of proton-decay studies since the discovery of the highly deformed proton emitters  $^{131}\text{Eu}$  and  $^{141}\text{Ho}$  [19]. Properties of excited states in deformed rare-earth nuclei allowed to extract the deformation and provide support for the single-particle configuration assignments for the proton emitting states. All elements between  $Z = 51$  and  $Z = 83$  but two have known proton emitters. Just above the  $Z = 50$  shells proton emitters are spherical or weakly deformed as one can see from

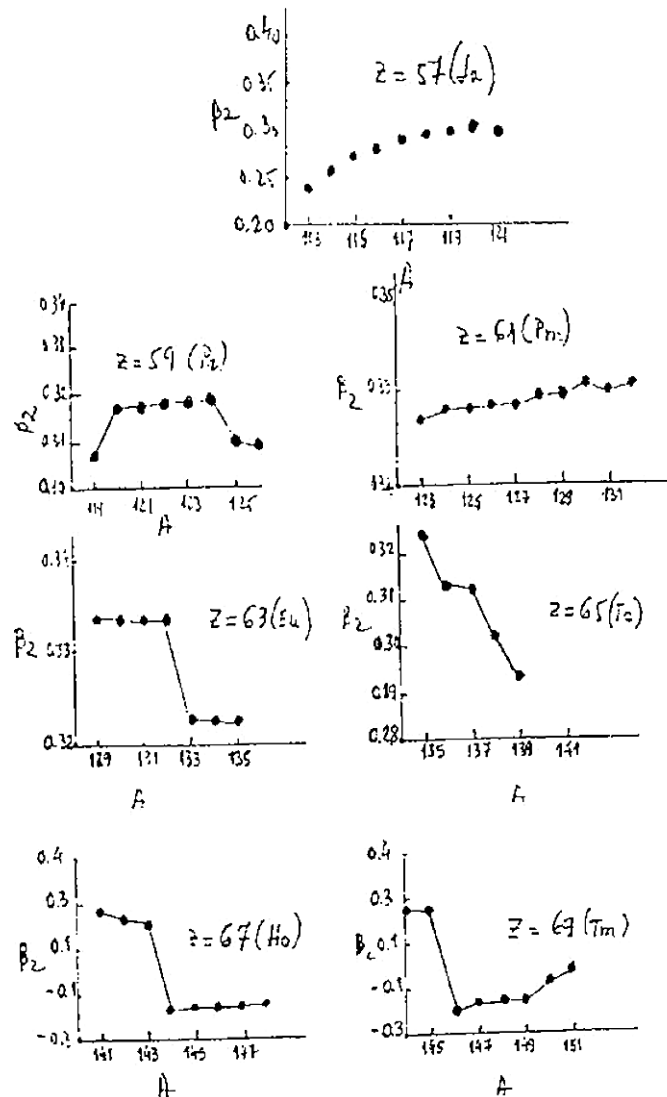
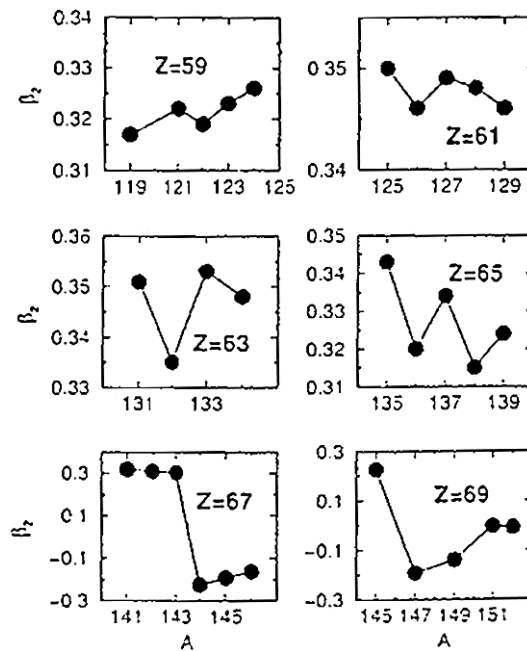


Fig. 10 – Self-consistent ground-state quadrupole deformations for the odd-Z nuclei  $57 \leq Z \leq 69$ .

Fig. 10; for heavier nuclei the proton drip-line enters the island of large prolate deformation in the middle of the  $Z = 50-82$  and  $N = 50-82$  shells. When approaching the  $N = 82$  shell calculated shapes change rapidly to oblate and then to spherical close to the  $N = 82$  line. The following discussion will be limited to the transitional nuclei with  $57 \leq Z \leq 69$ . The single-particle orbitals  $3/2^+[411]$ ;  $5/2^+[413]$ ;  $7/2^-[523]$ ;  $1/2^+[411]$  are predicted to constitute the ground state in Eu, Tb, Ho and Tm isotopes, at deformation between  $\beta_2 = 0.25$  and  $\beta_2 = 0.30$ . Below  $\beta_2 = 0.25$  in the case of the  $h_{11/2}$  proton orbital Coriolis effects become important and the strong-coupling picture cannot be applied. It is worth noting, that according to the microscopic-macroscopic calculations [3] the deformation change from  $\beta_2 = 0.25$  in  $^{145}\text{Tm}$  to  $\beta_2 = -0.19$  in  $^{147}\text{Tm}$  and also the deformation changes from  $\beta_2 = 0.22$  in  $^{143}\text{Ho}$  to  $\beta_2 = -0.15$  in  $^{145}\text{Ho}$  (Fig. 10). The similar results have been obtained by using HFB [20] calculations (Fig. 11).

Fig. 11 – Self-consistent ground-state quadrupole deformations for the odd-Z nuclei  $59 \leq Z \leq 69$ .



Studies of excited states in deformed proton emitters require an efficient and very selective detection method. The most exotic proton emitters are produced with cross sections of the order of 100 nb. The total reaction cross section is about 500 mb. Assuming 20  $\gamma$  rays per reaction, one  $\gamma$  ray out of  $10^8$  has to be selected to study excited states in the most exotic proton emitter. Recoil-Decay Tagging is the method of choice for studies of excited states in proton emitters. The method was used for the first time in connection with an array of Germanium detectors. The

RDT method can only be used for nuclei with proton and  $\alpha$  decay. In most of the cases, excited states in nuclei in the immediate vicinity of the proton emitter are not known. To fill this gap other methods have to be used. The best option at the moment to select weak reaction channels is the detection of light particles evaporated after heavy-ion fusion evaporation reactions. The measurements of  $^{130}\text{Eu}$  (Fig. 12) and  $^{135}\text{Tb}$  (Fig. 13) obtained at Argonne suggest that it will be possible to access all the proton emitting elements of light rare-earth nuclei.

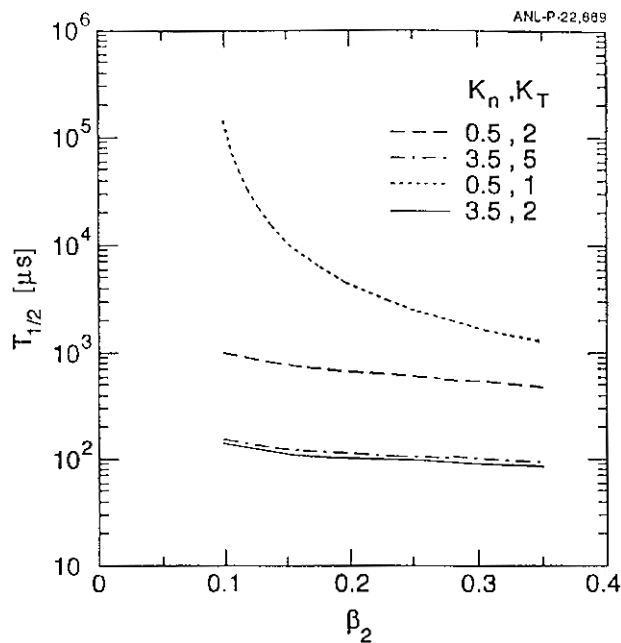


Fig. 12 – The measured proton decay half-life of  $^{130}\text{Eu}$  compared with calculation for proton emission from deformed odd-odd nuclei.

By using these methods excited states in  $^{147}\text{Tm}$  were observed in one of the first RDT experiments [19] with the modest array of Ge detectors AYEB coupled with a FMA (Fragment Mass Analyzer). The  $\gamma$ -ray coincidence spectra obtained in this experiment were assumed to form a band. The  $\gamma$ - $\gamma$  coincidences measured in the second experiment confirmed this hypothesis as can be seen in Fig. 14. The energies of the transitions indicate their quadrupole character. The band was interpreted as the  $h_{11/2}$  decupled band. These transitions could constitute the extension of the  $h_{11/2}$  band, or may come from a side band.

The observation of anomalous proton-decay rates in  $^{141}\text{Ho}$  and  $^{131}\text{Eu}$  motivated a search for their excited states. Compared to  $^{147}\text{Tm}$  the cross sections are about a factor 100 smaller. The results of the  $^{141}\text{Ho}$  study and a detailed discussion can be found in Ref. [21].

Fig. 15 shows the deduced moments of inertia from the ground-state band and the band based on the isomeric state in  $^{141}\text{Ho}$ . According to the Nilsson model

Fig. 13 – A comparison of the measured proton decay half-life of  $^{135}\text{Tb}$  with calculations assuming a highly prolate deformed shape.

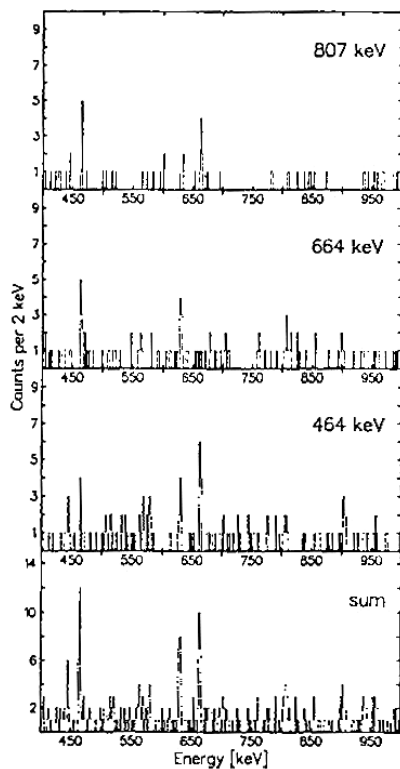
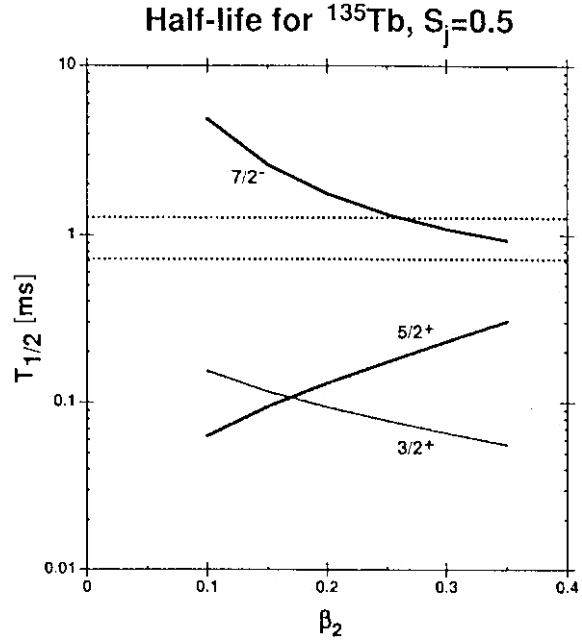


Fig. 14 – Proton tagged  $^{147}\text{Tm}$   $\gamma$ -ray spectra in coincidence with 464 keV, 664 keV and 807 keV transitions. The bottom panel contains the sum of the three gates.

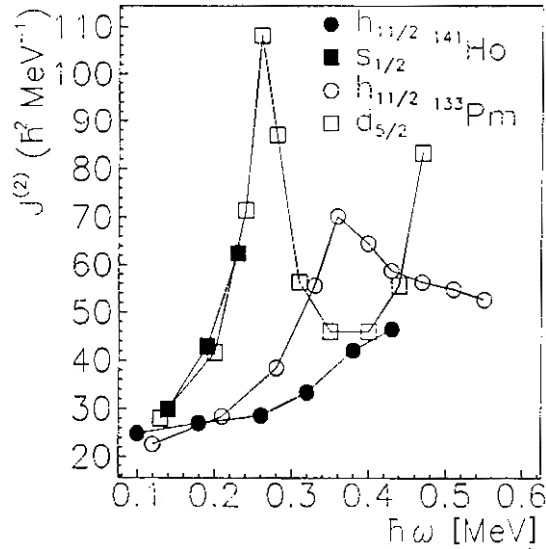
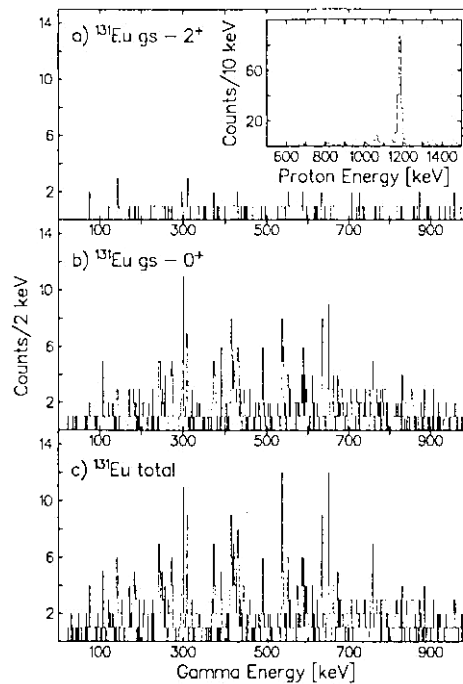


Fig. 15 – The dynamic moment of inertia deduced for the ground-state band and the isomer band in  $^{141}\text{Ho}$  are compared with the  $d_{5/2}$  and  $h_{11/2}$  bands in  $^{133}\text{Pm}$ .

Fig. 16 – The  $\gamma$ -ray spectra correlated with the ground-state  $^{131}\text{Eu}$  proton decay a) to the  $2^+$  excited state in the daughter nucleus, b) to the ground state and c) the sum. The inset shows the proton spectrum.



the  $7/2^- [523]$  configuration is the ground state in  $^{141}\text{Ho}$  at the calculated deformation of  $\beta_2 = 0.29$ . Adiabatic proton-decay calculations confirm this assignment and suggest the  $1/2^+ [411]$  orbital for the isomer. The analysis of the moment of inertia as a function of rotational frequency support these assignments. The first band

crossing due to the alignment of the  $h_{11/2}$  proton pair is blocked in the ground-state band. Using the Harris formula for the dynamic moment of inertia a deformation of  $\beta_2 = 0.25$  was deduced for the ground-state band. The detailed comparison of the ground state band level energies with particle – rotor model calculations indicates the need to include hexadecapole deformation and triaxiality.

The  $\gamma$ -ray spectra tagged with the  $^{131}\text{Eu}$  ground-state proton decay and the decay to the  $2^+$  excited state are shown in Fig. 16a and b, respectively. The large number of  $\gamma$  rays in the spectrum indicates that at least three bands were populated with comparable intensity. According to the Nilsson model the  $1/2^+$  [413] and  $3/2^+$  [411] orbitals are situated close to the Fermi surface in  $^{131}\text{Eu}$ . Based on a comparison with systematics of rotational bands built on top of the  $5/2^+$  [431] and  $3/2^+$  [411] levels on the other side of the  $N = 82$  line, the lowest transitions in the bands should be around 50 keV and 110 keV, respectively. The 72 keV  $\gamma$ -ray line present in the  $^{131}\text{Eu}$  spectrum favors the  $3/2^+$  [411] assignment. Similarities between the spectra correlated with the ground-state to ground-state proton line and the fine structure line confirm that the two lines are indeed emitted from the same state.

### THE PARTICLE – ROTOR MODEL

Rotational bands in odd-A nuclei, including odd-Z proton emitter, can be calculated using the Particle Rotor Model. The results of such calculations depend on the choice of input parameters. Due to a large number of parameters, which are not known very well and are very often strongly correlated the parameter space should be constrained to enable meaningful comparison with experiment. In the calculation performed for the  $^{141}\text{Ho}$  ground-state band a Woods-Saxon potential with the universal set of parameters was used to obtain single-particle energies. To take into account the effects of pairing the single-particle states underwent the BCS treatment. A proton pairing strength of 0.136 MeV was used in the calculations. As in other regions of the chart of nuclei the Coriolis interaction strength was attenuated by 15%. To illustrate the dependence of the calculations on different input parameters the calculated energies for the  $7/2^-$  [523] band in  $^{141}\text{Ho}$  are shown in Fig. 17. It can be seen that decreasing the quadrupole deformation, increasing negative hexadecapole deformation, increasing negative  $\gamma$  deformation facilitates transition to the decoupling regime marked by a rapid decrease in the energy of the  $11/2^-$  and  $15/2^-$  states with respect to the other states. For small  $\beta_2$  the splitting between different K orbitals decreases, which enhances K – mixing. For larger  $\beta_4$  values single-particle states are compressed and the mixing increases as well. The non-axial degree of freedom brings in additional  $\Delta K = 2$  mixing. Obviously, increasing the Coriolis strength has the same effect. It is worth noting that changing

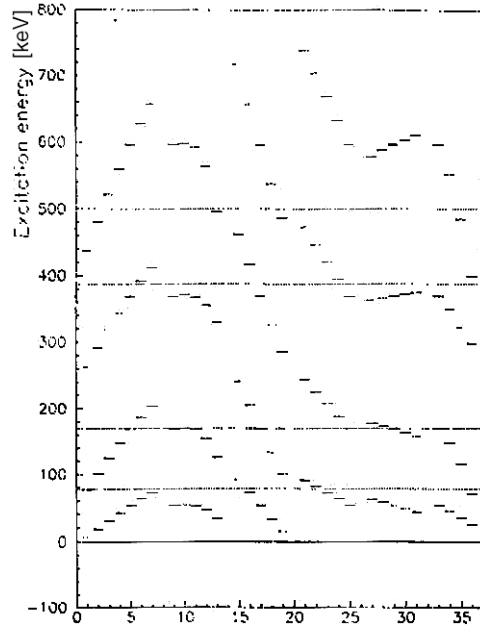


Fig. 17 – The calculated energies of the  $9/2^-$ ,  $11/2^-$ ,  $13/2^-$ ,  $15/2^-$  levels of the  $7/2^-$  [523] band in  $^{141}\text{Ho}$ , relative to the  $7/2^-$  band head, as a function of (from left to right):  $\beta_2 = (0.25, 0.26, 0.27, 0.28, \underline{0.29}, 0.30, 0.31)$ ,  $\gamma = (0^\circ, -5^\circ, \dots, -20^\circ)$ , pairing strength = (110%, 105%, 100%, 95%, 90%), Coriolis attenuation = (100%, 97.5%, 95%, 92.5%, 90%),  $E(2^+) = (\underline{180}, 190, 200, 210, 220 \text{ keV})$ ,  $\beta_4 = (\underline{0.00}, -0.02, -0.04, -0.06)$ . Only one parameter was varied at a time. Remaining parameters were fixed at the underlined values. The horizontal lines correspond to the measured level energies.

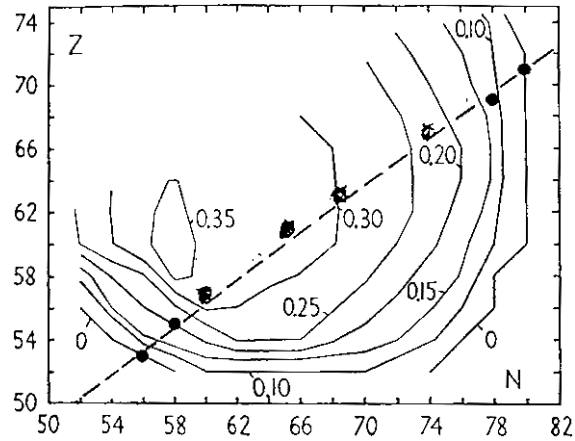
the pairing strength has a very strong effect on level energies. It is primarily because the Coriolis matrix elements are attenuated by a pairing factor which depends sensitively on the pairing strength.

## CONCLUSIONS

The present paper reports on some of the more recent results that we obtained in the study of light rare-earth nuclei. In this frame we established that  $^{117}\text{La}$  has two p-decaying levels that populate the ground state of  $^{116}\text{Ba}$ ; the ground state with  $J^\pi = 3/2^+$  decays *via* a  $(783 \pm 6) \text{ keV}$  proton with  $T_{1/2} = (22 \pm 5) \text{ ms}$ , while the excited level, with  $E_x = 150 \text{ keV}$  and  $J^\pi = 9/2^+$ , decays with  $E_p = (933 \pm 10) \text{ keV}$  and  $T_{1/2} = (10 \pm 5) \text{ ms}$ . A direct  $\gamma$  decay of the  $^{117}\text{La}$  excited level to the ground state would proceed through an M3 transition whose partial half-life would be 3.5 *s.i.e.* 350 times slower than the measured p-decay. Since our data do not show evidence of  $\alpha$  decays and a possible  $\beta$  decay would have  $T_{1/2}^\beta \sim 400 \text{ ms}$ , we attribute 100% branching to each of the two p-decays. Calculations performed for a deformed proton emitter reproduce quite well the experimental results confirming that  $^{117}\text{La}$  is strongly deformed ( $\beta_2 = 0.3$ ).

Our search for  $^{123}\text{Pr}$  and the studies of proton radioactivity of  $^{121}\text{Pr}$  emphasised that the proton drip line is shifted to lower neutron number for this nucleus.

Fig. 18 – Contour map of positive deformation  $\epsilon_2$  proton number  $Z$  and neutron number  $N$ . The figure is taken from D. A. Arseniev, A. Sobiczewski and V. G. Soloviev, Nucl. Phys. A, 126, 15, 1969 but the proton drip line was replaced by a straight line through the known proton emitters  $^{109}\text{J}$ ,  $^{113}\text{Cs}$ ,  $^{117}\text{La}$ ,  $^{126}\text{Pm}$ ,  $^{131}\text{Eu}$ ,  $^{141}\text{Ho}$ ,  $^{147}\text{Tm}$  and  $^{151}\text{Lu}$ . The figure exhibits three regions where nuclear structure has different influence on proton transitions. In region I around  $^{109}\text{J}$  and  $^{113}\text{Cs}$  the deformation changes rapidly and the contour lines are crossed by the proton transitions  $Z + 1, N \rightarrow Z, N$ . In region III between I and II, proton transitions are between nuclei of similar but large deformations.



For  $^{126}\text{Pm}$  our conclusion is that one needs a higher statistics run to be able to draw a firm conclusion on its decay nature .

Of course a fast decay is always possible and can not be discarded. The indication of the existence of  $^{130}\text{Eu}$  produced *via* a  $1p5n$  fusion evaporation channel and  $^{135}\text{Tb}$  representing the first example of a proton decaying isotope produced *via*  $1p6n$  evaporation channel obtained at Argonne suggest that it will be possible to access all the proton emitting elements of light rare-earth nuclei.

*Acknowledgments.* We would like to acknowledge the excellent technical help of Legnaro-team in setting up the whole experiment. This work was supported in part by the Romanian CERES project (C1-91) and by the European Community under LSF Contract. Our thanks to Mrs V. Braguta for her precise and professional work.

## REFERENCES

1. C. N. Davies *et al.*, Proc. Int. Conf. On Exotic Nuclei on Atomic Masses, Arles, France, 19–23 June 1995.
2. P. J. Wood *et al.*, 6-th Int. Conf. on Nuclei far from Stability, 1992.
3. P. Möller *et al.*, Atomic Data and Nuclear Data Tables, 59 (1995)185.
4. T. Faesterman *et al.*, Phys. Lett. 137B (1994), 23.
5. P. I. Sellin *et al.*, Phys. Rev., C47 (1993), 1993.
6. K. D. Page *et al.*, Phys. Rev. Lett., 68 (1992), 1287.
7. V. D. Bugrov and S. G. Kadmsky, Yad. Fiz., 49, 1562 (1989).
8. E. Maglione, L. S. Ferreira and R. J. Liotta, Phys. Rev., C59, R589 (1999).
9. K. Rykaczewski *et al.*, Phys. Rev., C60, 011301 R (1999).
10. L. S. Ferreira and E. Maglione, Phys. Rev. Lett., 86, 1721 (2001).
11. G. Audi *et al.*, Nucl. Phys. A624, 1 (1997).
12. S. Liran and N. Zeldes, At. Data Nucl. Data Tables, 17, 431 (1976).

13. J. Jänecke and P. J. Masson, *At. Data Nucl. Data Tables*, 39, 289 (1988).
14. G. L. Poli, Ph.D. thesis, University of Milan, 1998.
15. L. S. Ferreira and E. Maglione, *Phys. Rev.*, C61, 021304 (R) 2000.
16. F. Soramel *et al.*, *Phys. Rev.* C63, 031304 (R) 2001.
17. P. M. Endt, *At. Data Nucl. Data Tables*, 26, 717 (1981).
18. P. Möller, J. R. Nix and K. L. Krats, *At. Data Nucl. Data Tables*, 66, 131 (1997).
19. C. N. Davids *et al.*, *Phys. Rev. Lett.*, 80, 1849 (1998).
20. D. Vretenar, G. A. Lalazissis and P. Ring, *Phys. Rev. Lett.*, 82, 4595 (1999).
21. D. Seweryniak *et al.*, *Phys. Rev. Lett.*, 86, 1458 (2000).
22. V. A. Karnaukho, D. D. Bogdanov and Petrov, *Proc. Int. Conf. on the Properties of Nuclei from the Region of Beta-Stability*, CERN, Geneva 1970, 457.
23. Sigurd Hoffmann, *Particle Emission from nuclei*, Ed. D. Poenaru and M. Ivascu, vol. II, chapter 2, p. 26–67.
24. D. D. Bogdanov, V. P. Bochin, V. A. Karnaukhov and L. A. Petrov, *Sov. J. Nucl. Phys.*, 16, 491, 1973.